

Delta band contribution in cue based single trial classification of real and imaginary wrist movements

Aleksandra Vuckovic · Francisco Sepulveda

Received: 17 May 2007 / Accepted: 29 March 2008 / Published online: 17 April 2008
© International Federation for Medical and Biological Engineering 2008

Abstract The aim of this study was to classify different movements about the right wrist. Four different movements were performed: extension, flexion, pronation and supination. Two-class single trial classification was performed on six possible combinations of two movements (extension–flexion, extension–supination, extension–pronation, flexion–supination, flexion–pronation, pronation–supination). Both real and imaginary movements were analysed. The analysis was done in the joint time–frequency domain using the Gabor transform. Feature selection was based on the Davis-Bouldin Index (DBI) and feature classification was based on Elman’s recurrent neural networks (ENN). The best classification results, near 80% true positive rate, for imaginary movements were achieved for discrimination between extension and any other type of movement. The experiments were run with 10 able-bodied subjects. For some subjects, real movement classification rates higher than 80% were achieved for any combination of movements, though not simultaneously for all six combinations of movements. For classification of the imaginary movements, the results suggest that the type of movement and frequency band play an important role. Unexpectedly, the delta band was found to carry significant class-related information.

Keywords Brain computer interface (BCI) · EEG · Motor tasks · Movement imagery · Right hand

A. Vuckovic (✉)
Centre for Rehabilitation Engineering, University of Glasgow,
Glasgow, UK
e-mail: avuckovi@eng.gla.ac.uk

F. Sepulveda
BCI Group, Computing and Electronic Systems Department,
University of Essex, Colchester, UK

1 Introduction

Brain computer interface (BCI) systems based on EEG recordings can be utilized for a broad range of applications, from a long term use to assist communication in locked-in patients, driving a wheelchair and giving a command to a neural prosthesis, to short term applications for therapeutic treatment in rehabilitation and in different brain disorders [24]. The main advantages of EEG based BCI systems are that they are non-invasive, easy to use and relatively inexpensive. The main drawback of such BCI over more invasive recording is the low signal to noise ratio and low spatial resolution.

Motor imagination is often used for BCIs as it can utilize the cortical somatotopic representation of different parts of the body. However, this kind of BCI has typically been limited to four classes corresponding to four different parts of the body, such as left and right hand, both legs and tongue [23, 30]. The main difficulty in detecting different movements of the same limb, especially different movements about the same joint, is that they all activate nearly the same area of the motor cortex. Therefore, there have been only a few attempts to detect different real movements of a single limb from EEG recordings [6, 7, 19, 28, 33].

In the present study, a method for two class single trial classifications of both imaginary and real wrist movements were proposed. Different combinations of movements were classified in order to find which combination of movements would give the best classification results. Classification of different movements of the same wrist should increase the number of separable classes available for a BCI system (especially if used in combination with movements of different limbs) and should also enable more intuitive prosthesis control.

2 Methods

2.1 The experimental procedure

Ten neurologically healthy volunteers (8 men and 2 women, mean age 27.3 ± 7.8) participated in the study. All subjects signed a consent form based on the University of Essex's Ethical Committee recommendations. Subjects were comfortably seated on an armchair, their nose tips approximately 1 m from the computer screen, with the forearms on the armrest. They were asked to perform four types of real and kinaesthetic (i.e., the subject feels his/her limb executing a given action without visualizing the movement) imaginary right wrist movements that would correspond to rotation of the wrist around two axes: extension (E)/flexion (F), and pronation (palm down P)/supination (palm up S). For practice, prior to starting to record the EEG, the subjects had one full training session (approximately 12 min) of real movements and half of a session of the imaginary movements. During the experiment, real and imaginary movements were separated in different sessions. Each subject performed three sessions of real movements and four sessions of imaginary movements in the following order: real, imaginary, real, imaginary, real, imaginary, imaginary. Each session consisted of 15 repetitions of 4 different movements (E, F, P and S, in random order), 60 movements in total. Hence, each subject performed 180 real and 240 imaginary movements. The purpose of the real movement sessions was to help the subject to imagine the kinaesthetic movements later. Each session lasted about 12 min and the break between the sessions was between 5 and 15 min to allow the subject to rest.

At $t = 0$ s, a blank screen was presented to the subject (Fig. 1). At $t = 1$ s, a warning sign (a rectangle) appeared for 0.25 s on the screen. At $t = 2$ s, an arrow of 5 cm length, pointing right (E), left (F), up (P) or down (S) stayed for 3 s on the screen, i.e., until $t = 5$ s. The arrow indicated the movement to be executed (letters in parenthesis above). During that time, the subject was asked to keep the hand in a required position, i.e., to perform a sustained movement, whether real or imagined. The time between the arrow's disappearance and the new warning

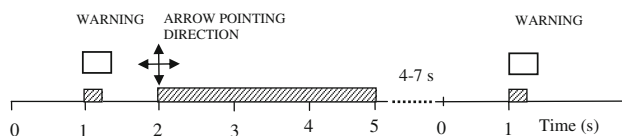


Fig. 1 Imagination protocol. A warning sign was presented 1 s before an arrow that indicated the type of movement. The duration of the warning sign was 0.25 s and the arrow was shown for 3 s. Meaning of arrow directions: *right* extension, *left* flexion, *up* supination, and *down* pronation

was random between 4 and 7 s. The total time between two trials was between 9 and 12 s.

2.2 Data recording

The electroencephalogram was recorded using a 64 channel BiosemiTM ActiveTwo system. Electrode placement was done according to the Biosemi ABC system, which, for 64 electrodes, corresponds to the international 10–10 system [1]. The ActiveTwo System has a preamplifier stage on the electrode and can correct for high impedances (in the range of 100 kOhm), so impedance measurements are not necessary. Nonetheless, the offset voltage (between the A/D box and the body) was kept between 25 and 50 mV, as recommended by Biosemi. The EEG amplitude was kept within 50 μ V. The system has 8 additional monopolar electrodes (called EX here) for measuring potentials from the other parts of the body. The reference electrode for EEG recording was an EX electrode placed on the right ear. All electrodes had the same ground. Electro-oculograms (EOGs) were recorded from the *orbicularis oculi*, from the outer cantus of the right eye, and below the right eye. EMG was bipolarly recorded during real and imaginary movements with two pairs of EX electrodes placed 2 cm apart on the *flexor carpi* and *extensor carpi* [10]. In that way, it was possible to determine whether there was any real movement during imaginary movement sessions. Also, to detect the onset of muscle activity, EMG was rectified and averaged over 30 ms [11]. The criterion for movement onset was that the averaged EMG while the arrow was on a screen exceeded mean \pm ($2 \times$ SD) of the averaged EMG from the first 50 ms of the reference period (the reference period started 1 s before a warning sign, that had no muscle activity related to the analysed movement) [11].

2.3 EOG removal using independent component analysis

EOG artefact was minimized using independent component analysis (ICA) as described in [13]. ICA components were compared with EOG and components that included EOG were set to zero before inverting the data to the EEG domain.

2.4 Data pre-processing

The raw EEG was referenced to the right ear and filtered (Butterworth filter of the 5th order, high pass cut off frequency at 0.5 Hz and low pass cut off frequency at 90 Hz). The highest frequency of interest was three times lower than the sampling frequency, as recommended by [2]. In addition, a Butterworth stopband filter was applied at 50 Hz. To obtain a reference-free recording, a Laplacian

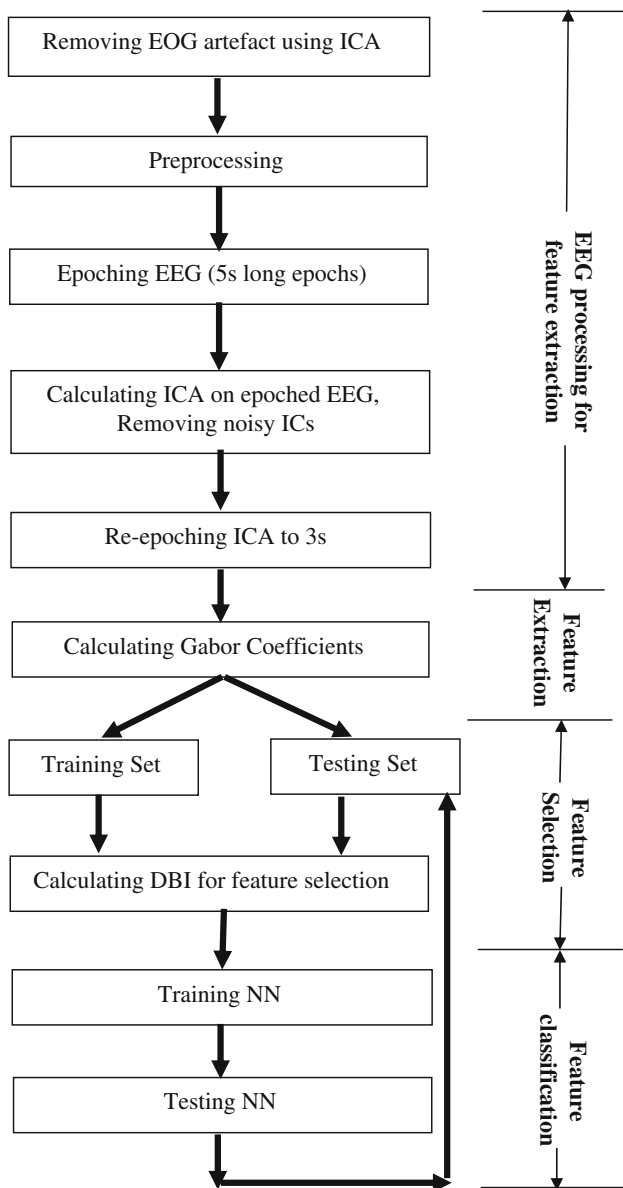


Fig. 2 Flow chart of the overall analysis procedure

was computed based on [12] that included the center and the four nearest electrodes (three nearest electrodes for electrodes at the edge). A flow chart showing the signal processing procedure is shown in Fig. 2.

2.5 Calculating independent components for feature extraction

EEG signals at nearby points of the scalp tend to be correlated. This effect is not very pronounced if the recording electrodes are relatively far from each other, such as when different limb movements are analysed. However, if the recording electrodes of interests are close to each other, it

is desirable to de-correlate the underlying sources as much as possible. Therefore, in this study, before applying feature extraction, the EEG was replaced with its independent components.

Epochs were extracted from the EEG signals after EOG artefact removal. An epoch started at $t = 0$ s and finished at $t = 5$ s, when the arrow disappeared from the screen (see Fig. 1 above). A reference period was determined in which there was no activity related to the movements i.e., from $t = 0$ s to $t = 1$ s. The baseline value (i.e., the mean value of 50 ms EEG at the beginning of the reference period) was subtracted from the whole epoch to avoid low frequency drifts. Independent components were calculated again based on epoched EEG, according to Eq. 1 below. To calculate the ICs, only the EEG channels were used. The Infomax algorithm was used [21] as implemented in open source Matlab Toolbox EEGLab [5]. EEG epochs were divided into four groups (EEG₁–EEG₄) according to the class of a movement. Independent components were calculated for one class of movement (separately for each subject) and the same transformation matrix was then applied to the other classes of movements. If the ICs were calculated independently for each class, it would not be possible to compare the ICs for two different classes for the corresponding locations because components obtained from different movements generally do not have the same numbering. Therefore IC₁ and the unmixing matrix W_1 were calculated only for one EEG set, hereby named EEG₁. The same unmixing matrix W_1 was then applied to the EEG₂₋₄ signals for the other three movements to calculate the IC₂₋₄ for those movements, as follows:

$$\begin{aligned} IC_1 &= W_1 \cdot EEG_1 & IC_2 &= W_1 \cdot EEG_{2_1} \\ IC_3 &= W_1 \cdot EEG_{3_1} & IC_4 &= W_1 \cdot EEG_{4_1} \end{aligned} \tag{1}$$

To avoid biased classification towards one class of movement, IC₁ was chosen so that each class from four possible classes was used at least twice. After calculating the ICs on 5 s epochs, the first two seconds were discarded and only the period from $t = 2$ s to $t = 5$ s remained. Thus IC sets contained only 3 s long epochs showing brain activity while the arrow was on the screen, i.e., EEG related to the movement.

IC components containing noise (i.e., segments that exceeded mean $\pm 3SD$ of the mean amplitude of the rest of the ICs) that was present in at least 25% of the epochs (i.e., it was present at least during one recording session) were excluded from the analysis, as suggested in [29]. The spatial location of the noisy components was checked using EEGLab and it typically corresponded to location of the electrodes that were recording a noisy raw signal. In that way, no epochs were excluded because of EOG or noise (only the corrupted IC components were removed, not the entire epoch).

2.6 Time–frequency analysis

The discrete Gabor transformation (DGT) was applied to the ICs to calculate the Gabor coefficients (GCs). The Gabor transformation is a windowed Fourier Transformation with a fixed size of the windows in both time and frequency domain [18, 25]. The size of the window in this study was 120 ms in the time domain and 2 Hz in the frequency domain. The size of the window in the frequency domain was chosen to enable analysis of the alpha band. The 120 ms time window corresponded to time windows typically used to analyse ERD and ERS.

The windowing function used was the Gaussian function. In this study, only a direct DGT was applied to calculate the Gabor coefficients, as follows:

$$GC_{mn} = \sum_{k=0}^{L-1} IC[k] \gamma[k - m \cdot \Delta M] \exp\left(-jkn \frac{2\pi}{N}\right),$$

$$- \Delta N < m < \Delta N \quad 0 \leq n \leq \Delta M - 1$$

$$\gamma[k] = \sqrt{\frac{\sqrt{2}}{T_1}} \cdot e^{-\pi \left(\frac{k - 0.5(N_1 - 1)}{T_1}\right)^2} \quad 0 \leq k \leq N_1 - 1,$$

$$T_1 = \sqrt{\Delta M \cdot N}, \quad (2)$$

where IC are the independent components, γ is the analysis Gaussian function, $N_1 = 256$ is the number of samples in the analysis function (and at the same time it is the number of grid points in the time and frequency dimension), $\Delta M = 32$ is the time step, $\Delta N = 2$ is the frequency step, i.e., the bandwidth, and $N = 128$ is the number of frequency steps ΔN in the frequency dimension [18]. Although GCs are complex, only the absolute value of the GCs corresponding to 0.5–90 Hz (45 frequency bands, width of each band 2 Hz) were included for the analysis in this study. In that way the delta, theta, alpha, beta and gamma ranges were taken into account.

2.7 Feature selection using the Davis-Bouldin index

The total number of GCs calculated as described above was large. For example, for 64 ICs there were $64 \cdot 25 \cdot 45 = 72,000$ Gabor coefficients per epoch, where 25 is the number of 120 ms wide time windows and 45 is the number of 2 Hz wide frequency bands. Therefore, it was necessary to find which features (GCs) were the most distinctive between different types of movements. The Davis-Bouldin index (DBI) was used to estimate overlapping between any two classes (i.e., paired combinations of four different wrist movements) based on the absolute values of the Gabor coefficients. The DBI is a function of the sum of within-cluster scatter to between-cluster separation [3]. DBI has already been used for classification of biological signals, like EMG and EEG [27, 34]. In this

study, the DBI was used for EEG class separation as described in [27]. The numerical values of the DBI are proportional to the degree of class overlapping. A small DBI value for one feature means that that feature has very distinctive values for different classes, which corresponds to good class separation.

An optimum number of features for the given data set cannot be estimated a priori but had to be tested empirically. In general, an insufficient number of features or too large number of features (i.e., including features with a big degree of overlapping) would result in poor separation. Features selected according to their minimum DBI and used for classification will be called “relevant features” in the text.

As already mentioned, spatial information for different movements was poor and could not be utilized. Therefore choosing small time-frequency windows (2 Hz and 120 ms) was necessary in order to capture small differences between different types of movements. However for such small time-frequency windows features can be highly nonstationary. To solve this problem, DBIs were calculated for each feature five times, on a randomly chosen subset of the training set, containing each time 50% of the whole training set. Every time each feature was ranked and an average DBI value was calculated. Feature selection was then based on the average rank values of the DBI indexes.

2.8 Feature classification

2.8.1 Neural networks

Although the DBI index gives information about the relevance of features, it is still necessary to apply a classifier to discriminate between the different movement classes. As the focus of the current study was on defining the frequency and temporal distribution of features that are distinctive among different classes of movements about the same joint, and not on investigating which classifier would be best for the task, only two types of supervised NN were applied, one feed forward and the other recurrent. Elman networks (ELMNN) [8] were used for feature classification, as they were already proven to be successful for discrimination between different mental tasks [22]. The ELMNN was trained with gradient descent with momentum and the adaptive learning rate backpropagation algorithm. The stopping criterion was $MSE = 0.015$.

The feed-forward network we used was a multi-layer perceptron (MLP). Similar to the ELMNN, the MLP was trained with the adaptive learning rate backpropagation algorithm and had the same stopping criteria ($MSE = 0.015$) and output rating criteria. The MLP was chosen because it had the same training algorithm and transfer functions as the recurrent network.

Before training the networks, all weights in the hidden layer were given random values in the range between the smallest and the largest values of the network input based on the whole training set. The output rating criteria were ‘winner takes all’ for both networks. To exclude the possibility that the recurrent network learns the order in which different classes were presented, rather than the class itself, the order of presentation of the different classes was different in the training and the testing sets, but was the same for both networks.

2.8.2 Training and testing set

A feature set consisted of absolute values from the GC calculated on the 0.5–90 Hz range. A training set consisted of 2/3 of the data and the testing set consisted on the remaining 1/3 of the data. For each subject, both networks were trained on 10, 25, 40, 50, 60, 75, 100, 150, 200, 300, 400 and 500 features with the lowest DBIs.

For the imaginary movements, training and testing was performed on 10 subjects. Training sets had 40 trails and testing sets had 20 trials. For the real movements, classification was performed on 4 subjects only due to EEG recording availability problems. Training sets consisted of 30 trials and testing sets consisted of 15 trials.

Each subject performed four different types of wrist movements. When two different movements were classified, there were six possible combinations:

1. Extension–Flexion (EF)
2. Extension–Supination (ES)
3. Extension–Pronation (EP)
4. Flexion–Supination (FS)
5. Flexion–Pronation (FP)
6. Supination–Pronation (PS)

2.9 Statistical analysis

Kruskal-Wallis nonparametric one-way analysis of variance was performed to test whether there was a statistically significant differences between any of the groups. After that, for each pair the Wilcoxon rank-sum test was performed to test for statistically significant differences.

3 Results

3.1 Classification of two different right wrist imaginary movements

Classification results using ELMNN for all six combinations of imaginary movements, for all ten subjects, are shown in Table 1. The training step preceded in time the

Table 1 True positive rate classification of two imaginary movements with ELMNN for six different combinations of movements

Subject	Ext–Flex	Ext–Pro	Ext–Sup	Flex–Pro	Flex–Sup	Sup–Pron
1	100	96	93	72	65	61
2	92	92	85	66	61	58
3	87	92	82	56	61	61
4	87	82	78	64	67	67
5	83	83	77	50	67	58
6	87	82	77	50	67	64
7	77	82	77	58	67	72
8	77	72	72	42	59	55
9	82	77	67	61	56	67
10	53	53	83	56	77	64
Mean	82 ± 12	81 ± 12	79 ± 7	58 ± 9	65 ± 6	63 ± 5

testing set as this is a prerequisite for an on-line application such as a BCI.

There were statistically significant differences between classification rates for the six different pairs of movements (Kruskal Wallis test $P = 2.4144 \times 10^{-6}$). The best classification results were achieved when extension was one of the movements that were classified. There was no statistically significant difference between the classification rate for any of the combinations of EF, EP and ES (EF vs. EP, EF vs. ES and EP vs. ES, Kruskal Wallis test $P = 0.434$) but there was a statistically significant difference in the classification rate between any of EF, EP or ES and any of FP, FS or SP (nine combinations in total). There was also a statistically significant difference between the classification rates of FP versus FS. In most cases, up to 150 features (out of 72,000) were sufficient to obtain a good classification. In many cases, classification rates higher than 80% were achieved with as few as 10 features with the lowest DBI. Increasing the number of features over 100 decreased in most cases the classification accuracy, probably because most features do not contain class-related information.

In addition, the ELMNN network was trained on each of three combinations of 2/3 of the set and tested on the remaining 1/3 of the data. The results for EF, EP and ES, that achieved the highest classification accuracy in the previous example are shown in Table 2. Classification rates were similar to those in Table 1.

A feed-forward network was trained to classify imaginary flexion versus imaginary extension. The first 2/3 of the data were used for training and the remaining 1/3 of the data was used for testing. Results are shown in Table 3. The average classification rate was 78 ± 12 . That is 4% less than the average classification rate for the ELMNN. Still, these classification results are relatively high for the single-joint scenario, showing that the features are separable even with a simple neural network. An important

Table 2 Mean value of true positive rate for classification of two real movements with ELMNN for different combinations of movements

S	1	2	3	4	5	6	7	8	9	10
EF	96 ± 4	90 ± 2	89 ± 3	83 ± 3	82 ± 1	81 ± 1	79 ± 3	75 ± 3	83 ± 2	52 ± 1
EP	95 ± 2	95 ± 2	95 ± 2	95 ± 2	95 ± 2	95 ± 2	95 ± 2	95 ± 2	95 ± 2	95 ± 2
ES	96 ± 4	96 ± 4	96 ± 4	96 ± 4	96 ± 4	96 ± 4	96 ± 4	96 ± 4	96 ± 4	96 ± 4

Training set preceded in time the testing set

advantage of the ELMNN over the feed-forward NN was the computational speed. For the same parameters (number of features, hidden neurons, and training criteria) and for a larger number of features (>50), the ELMNN was trained more than 10 times faster (less than 1 min with the ELMNN compared to 10 min with the MLP all programs being executed in Matlab 7 on a PC Pentium 3.6 GHz with 1 GB RAM).

3.2 Classification of two different right wrist real movements

Table 4 shows classification results for six groups of two real wrist movements. While for the imaginary movements the best results were achieved for classification of extension versus other types of movements, such a tendency was not observed for the real movements. There was no statistically significant difference between the classification of all six different combinations of movements (Kruskal Wallis test $P = 0.9198$). Classification rates equal or higher than 80% were achieved for any combination of two real movements.

Table 3 True positive rate for classification between extension and flexion with feed-forward NN

Subj	1	2	3	4	5	6	7	8	9	10
Clas.	89	81	81	83	64	72	77	76	100	55
NF	25	60	75	75	10	10	10	25	25	60

Training set preceded in time the testing set

Table 4 True positive rate for classification of two real movements with ELMNN for six different combinations of movements

Subject	Ext–Flex	Ext–Pro Sup	Ext–Sup	Flex–Pro	Flex–Sup	Sup–Pron
2	61	61	77	83	77	77
4	83	86	75	61	56	47
5	60	90	85	90	85	80
6	75	57	70	54	100	57
Mean	70 ± 11	74 ± 17	77 ± 7	72 ± 17	80 ± 18	65 ± 16

S subject; EF extension–flexion; ES extension–supination; EP extension–pronation

However, for none of the subjects were good classification rates achieved for all six combinations of movements. The training sets for the imaginary movements were 33% larger than those for the real movements. Better classification results would be expected for classification of the real movements if the same sizes of the training sets were available. In all but one case 10 to 200 features were used and in one case (EP subject 4) 400 features were used.

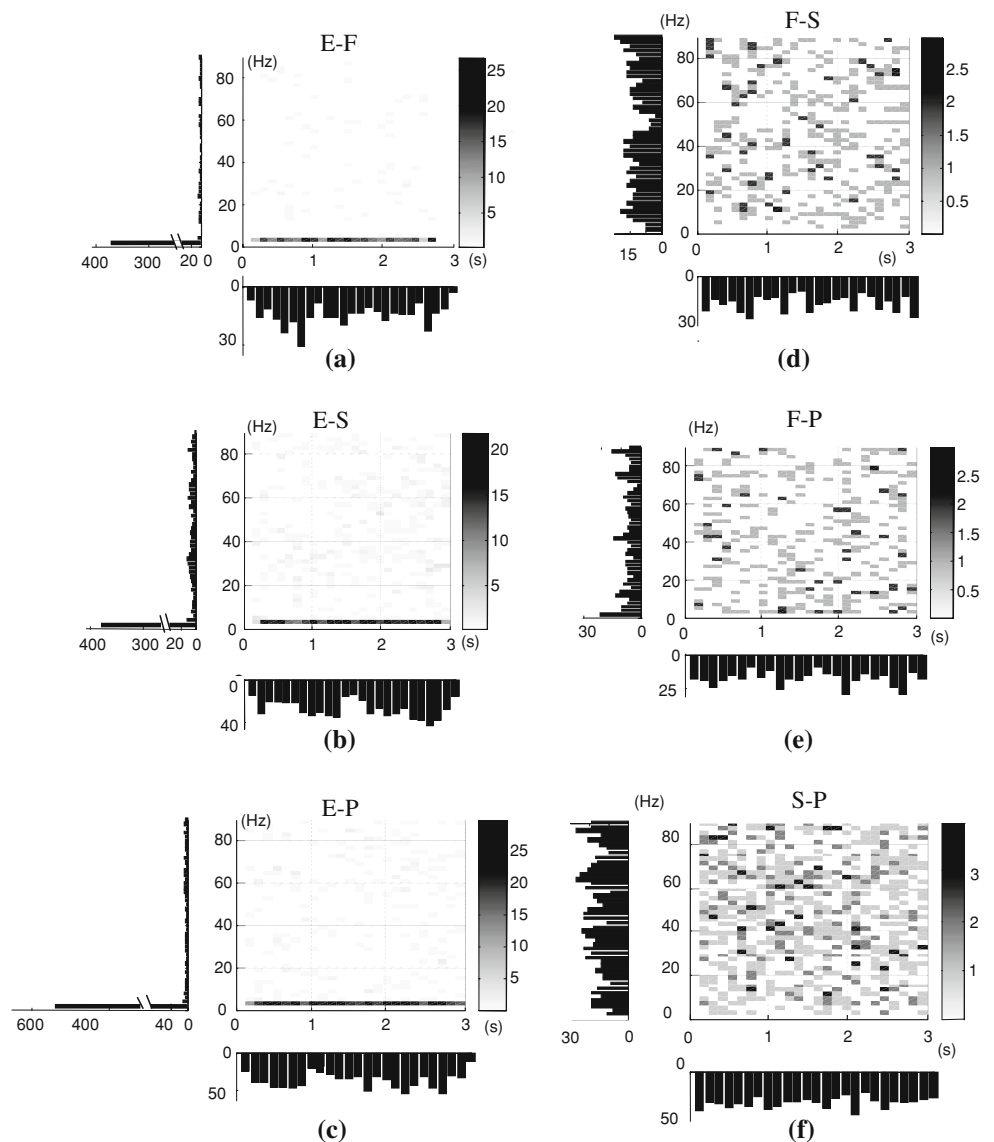
3.3 Temporal and frequency distribution of the features used for training

Figure 3a–f shows the distribution of features used for classification between two imaginary movements for all subjects in the time–frequency domain. The figures were obtained by summation of features over all subjects. All classifications that included extension as one of the movements had clearly dominant features in the delta band. In addition, for classification of flexion versus pronation, the lower delta band (0–2 Hz) contained the largest number of features per 2 Hz band. Although there was no averaging, but only summation across the subjects, from the total number of features and number of features per subject, it is evident that delta band features were dominant in all subjects. The temporal distribution of features in the delta band showed that, with the exception of the first 120 ms, the features were distributed in the whole 3 s range. However, the overall temporal distribution of the features for the E–F, E–S and E–P combinations showed the largest number of features in the first second and in the third second (close to the end of the sustained movement). The first second corresponded to movement preparation and execution. The increased number of features at the end of the third second might indicate preparation for a movement that should bring the hand back to the resting position, as it is possible that after a lot of repetition a subject could roughly predict the length of a 3 s period.

Figure 4a–f shows the distribution of features used for classification between two real movements. It is interesting to notice that for all six combinations of movements, there were many features outside of the alpha and beta bands.

There was a large number of features in the 0–2 Hz delta band for classification of E–F and E–S combinations. In the case of classification of E–P, F–S and S–P there were

Fig. 3 Time–frequency distribution of features used for classification of different combinations of imaginary movements. Features are summed up for all subjects. Marginal distributions were calculated by summing all the features for the given column or row. *E* extension, *F* flexion, *S* supination, *P* pronation



not many features in the delta band, but the largest number of features per 2 Hz band was in the theta band. Again, although figures present summed up features across the subjects, it can be noticed that the delta band features were not as dominant as for the imaginary movements, especially for E–S classification, although a relatively high average classification rate of 77% was achieved. For that combination of movements (E–S), there were many features in the higher gamma range (Fig. 4c). A large number of features in the theta and gamma range can also be noticed for F–S classification, resulting in a peak in the temporal distribution (Fig. 4d).

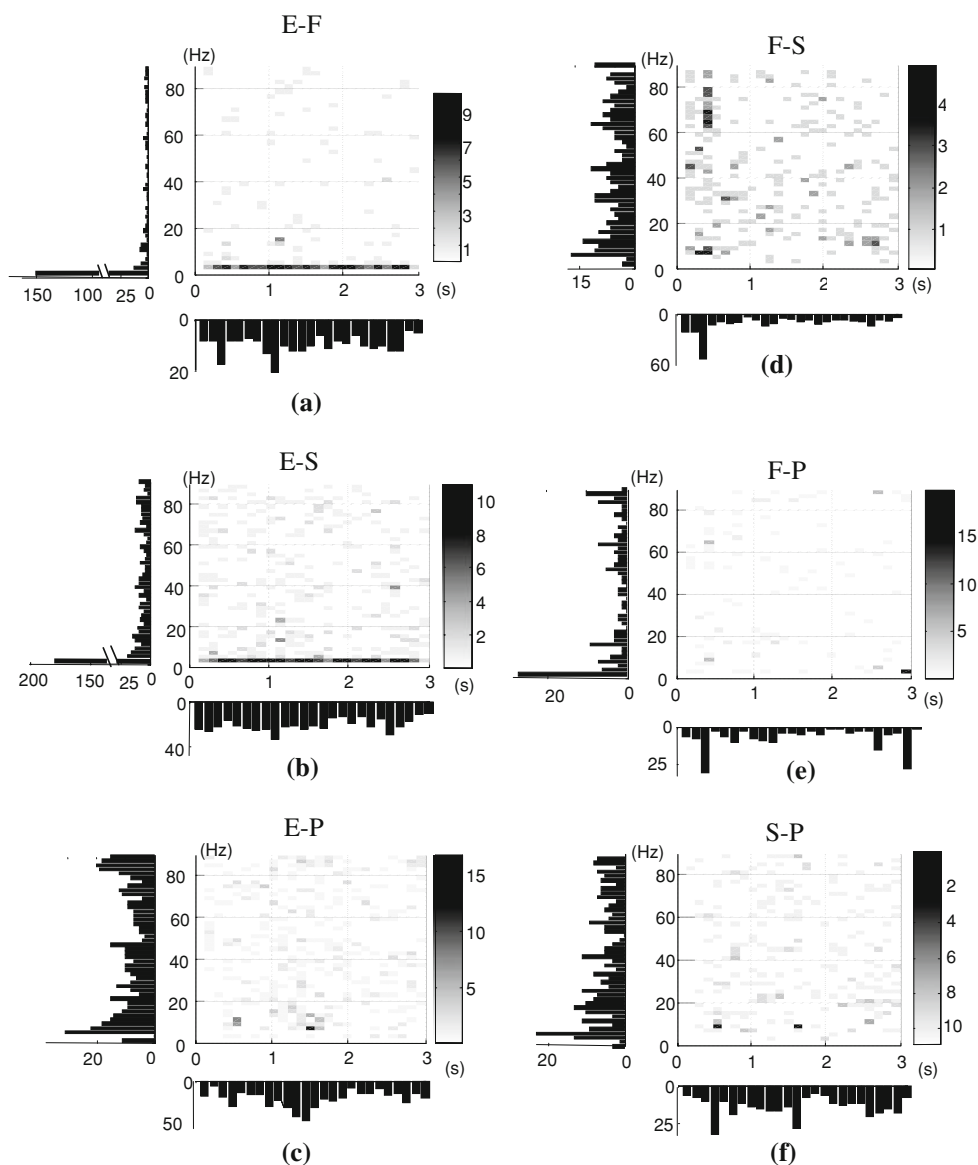
Regarding the temporal distribution of the features, a clear maximum could be noticed in the period at 240–480 ms after the cue onset (Fig. 4a, c–f), which would correspond to movement preparation and initialisation (based on EMG, a movement started 390 ± 90 ms after the cue onset for

extension, and 420 ± 120 ms for flexion). However, for classification of extension versus other types of movements, and for classification of supination versus pronation, the overall largest number of features was during the 2nd second, i.e., while the hand was in a required sustained position. There was also a clear peak during the 2nd second for F–P and a peak at the end of the 3rd second for S–P.

3.4 An example of spatial distribution of the independent components

Figure 5a, b shows spatial distributions of 3 ICA components with the overall largest number of relevant features, for classification of real and imaginary combinations of movements extension versus flexion, in subject 4. In this subject, both for imaginary and real movements, the best classification results were achieved for classification of

Fig. 4 Time–frequency distribution of features used for classification of different combinations of real movements. Features are summed up for all subjects. Marginal distributions were calculated by summing all the features for the given column or row. *E* extension, *F* flexion, *S* supination, *P* pronation



extension versus other types of movements. ICA components were chosen because when classification was performed with as few as 10 features, they typically belonged to no more than 3 different ICs. The pictures were generated in EEGLab by calculating for each IC the relative projection weight at each electrode [21].

The same transformation matrix was used to calculate ICs for all four movements (separately for real and imaginary movements). Therefore, calculated ICs have the same relative projection to each electrode, i.e. the same spatial location for all four movements. Therefore in some cases, the components with the same spatial location were used for classification of two different groups of movements. That is however not surprising because in all cases extension was included as one type of a movement. For imaginary movements, the ICs were not clearly localized in

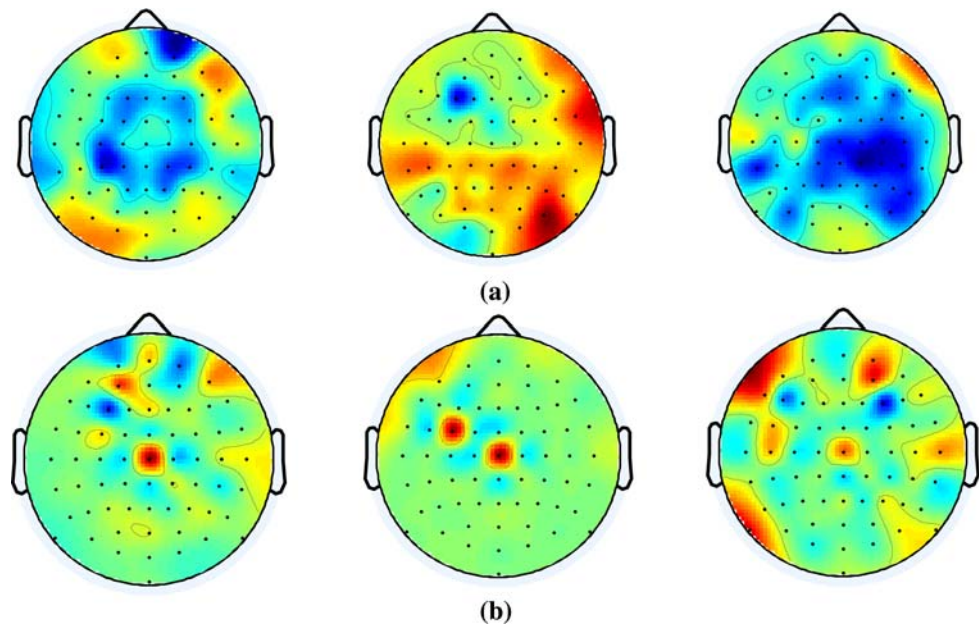
the sensory-motor area of the right hand. For example, the first component for the EF is located bilaterally over representation area of the both hands, while the third component for the EF is located over the ipsilateral hand area and over a larger ipsilateral parietal area. Because most of features belonged to the delta band, Fig. 5a virtually shows the distribution of delta band features.

For the real movements, ICA components seem to be much more localized and corresponded to electrodes position C_z and CF_3 and in the frontal area around AF_4 .

4 Discussion

This study presents results for two class separation of real and imaginary movements of the same wrist. Experiments

Fig. 5 Spatial distribution of three dominant ICs for classification of extension versus flexion, **a** imaginary and **b** real movements



were performed on naive subjects. For most of the classification examples in this study, 2/3 of data were used for training and 1/3 for testing, with training data preceding in time the testing data, which is a prerequisite for future on-line BCI applications [30].

A recent study on classification of imaginary movements of different limbs showed that applying ICA does not significantly improve the classification accuracy, compared to a Laplacian derivation [16]. In our study, a classification rate was not much higher than 50% (i.e. by chance) based on EEG signals with Laplacian derivation. When using ICA, the highest classification rate for the imaginary movements, around 80% was achieved for classification of extension versus any other type of imaginary movements (flexion, supination, pronation). In the case of high classification accuracy (>80%) the largest number of relevant features belonged to the delta range. This was a somewhat surprising result because that frequency range has not been considered in most of the studies based on motor imagery. However, Kauhanen et al. [14] achieved the best classification accuracy of right versus left imaginary hand movement in tetraplegics using EEG signals in the 0.5–3 Hz range. In an EEG-based study on influence of practice on motor imagination [17], even related desynchronisation/synchronisation (ERD/ERS) was noticed in the delta and theta band before training and a significant increase of ERD/ERS in these two frequency bands was noticed after training. In an ECoG study on finger tapping in subjects with no motor disorders, Graiman et al. [9] showed a clear correlation between the normalized band power changes in the delta, beta and gamma range and movement execution.

For the real movements, classification accuracy higher than 80% (up to 100%), was achieved for any of the six

combinations of movements in the current study. However, for each subject there were typically only 2–3 combinations of movements that could be classified with high accuracy. For classification of the real movements, there was a large number of relevant features in the delta band but some relevant features were found in other frequency bands as well.

Surprisingly, there was more consistency regarding the best classifiable type of movement and relevant frequency range for the imaginary than for the real movements. One possible explanation is that wrist extension was the easiest movement to imagine. However, further evidence is needed. In the current study, the spatial distribution of ICA components with the largest number of relevant features was more obviously concentrated around the contralateral motor area for the real movements than for the imaginary movements. A possible reason for this is that the subjects might have combined visual and motor imagery, as maximum EEG activity can be outside the sensory-motor area in visual imagery [20]. It is also interesting to note that relevant ICA components were sometimes distributed over the ipsilateral hand area for imaginary movements.

We performed another study on the same set of data but on averaged EEG signals instead on single-trial based ICA [33]. In that study, we calculated regions of significant ERD/ERS based on [35] and then looked at significant differences between ERD/ERS of two imaginary or real movements [33]. We calculated the energy based on the Gabor transformation in 240 ms and 2 Hz time–frequency windows, called resels as in [35]. The region of the largest differences between two movements in general was on Cp3 in the 12–30 Hz. Yet, for both real and imaginary movements, regions of significant differences were also found in

the theta and the delta band. Although significant resels in low frequency bands were found on all electrode locations, their number was the largest in the frontal region (premotor area coronal lines F and FC, and more frontal areas) and to a lesser degree in the parietal region, corresponding to the coronal line of P electrodes. It is hard to say whether activation of the frontal areas of the cortex corresponded to movement planning, visual processing of the cue on the screen (and would not appear in a self-paced BCI paradigm) or to a non-kinaesthetic movement imagination [20].

Similar to the current study, there was no clear time distribution of low-frequency resels in [33]. However, the total number of significant resels was larger than the total number of features used for classification in the current study, and it is difficult to determine whether features in 12–30 Hz band would be more significant than those in the delta and theta bands.

The classification rate was lower than for classification of imaginary right versus left hand movement presented in the literature [26] but the task in the present study was more complex as there was little spatial selectivity.

In the present study a sustained 3 s long, rather than repetitive or single fast movement was performed. For the imaginary movements, the largest number of features was found in the first second and for the real movements a clear peak could be noticed in a period 240–480 ms after the cue onset, that corresponded to movement preparation and initialisation.

Combining different movements of the same hand with movements of different hands (or different parts of the body in general) would lead to an increased number of separable classes. Classification of the left versus right hand can be already achieved with high accuracy even online and would not significantly increase the classification error [4, 31]. Combining 3 or 4 types of movements would increase the number of separable classes, but would decrease classification accuracy [32]. When choosing an optimum number of classes for a BCI system, a compromise should be made between the possible degrees of freedom and a classification accuracy [15]. Combination of classification of two different movements of the same hand and movements of different hands would give a reasonably high classification accuracy. In addition it would be more intuitive in applications that include neural prosthesis and upper limbs therapy, compared to BCI systems that classify imaginary movements of hands, legs and tongue.

5 Conclusion

This paper shows that it is possible to separate two different movements of the same wrist with an average

classification accuracy of 80%. This true positive rate was achieved for both real and imaginary movements. Further, most of the relevant features selected for classification of the imaginary movements belonged to the delta range.

Acknowledgments This work was supported by the EPSRC through Grant GR/T09903/01.

References

1. American Clinical Neurophysiology Society (2006) Guideline 5. Guidelines for standard electrode position nomenclature. *J Clin Neurophysiol* 23(2):107–110
2. American Clinical Neurophysiology Society (2006) Guideline 8. Guidelines for recording clinical EEG on digital media. *J Clin Neurophysiol* 23(2):122–124
3. Bezdek JC, Pal NR (1998) Some new indexes of cluster validity. *IEEE Trans Syst Man Cybern B Cybern* 28:301–315
4. Blankertz B, Dornhege G, Krauledat M, Müller KR, Kunzmann V, Losch F, Curio G (2006) The Berlin brain-computer interface: EEG-based communication without subject training. *IEEE Trans Neural Syst Rehabil Eng* 14(2):147–152
5. Delorme A, Makeig S (2004) EEGLAB: an open source toolbox for analysis of single-trial EEG dynamics including independent component analysis. *J Neurosci Methods* 134(1):9–21
6. Deng J, Yao J, Dewald JP (2005) Classification of the intention to generate a shoulder versus elbow torque by means of a time-frequency synthesized spatial patterns BCI algorithm. *J Neural Eng* 2(4):131–138
7. do Nascimento OF, Nielsen KD, Voigt M (2005) Influence of directional orientations during gait initiation and stepping on movement-related cortical potentials. *Behav Brain Res* 161(1):141–154
8. Elman JL (1990) Finding structure in time. *Cogn Sci* 14:179–211
9. Graimann B, Huggins JE, Levine SP, Pfurtscheller G (2004) Toward a direct brain interface based on human subdural recordings and wavelet-packet analysis. *IEEE Trans Biomed Eng* 51:954–962
10. Hermens HJ, Freriks B (1999) Surface electro-myography for non-invasive assessment of muscles recommendation European concerted action in the Biomedical Health and Research Programme (Biomed II) of the European Union. Recommendation for the recording of SEMG signal (CD-ROM)
11. Hermens HJ, Freriks B (1999) Surface electro-myography for non-invasive assessment of muscles recommendation. European concerted action in the Biomedical Health and Research Programme (Biomed II) of the European Union. Signal Processing Recommendation. (CD-ROM)
12. Hjort B (1975) An online transformation of EEG scalp potentials into orthogonal source derivations. *Electroenceph Clin Neurophys* 39:526–530
13. Jung TP, Makeig S, Westerfield M, Townsend J, Courchesne E, Sejnowski TJ. Removal of eye activity artifacts from visual event-related potentials in normal and clinical subjects. *Clin Neurophysiol* 111(10):1745–1758
14. Kauhanen L, Nykopp T, Lehtonen J, Jylänki P, Heikkonen J, Rantanen P, Alaranta H, Sams M (2006) EEG and MEG brain-computer interface for tetraplegic patients. *IEEE Trans Neural Syst Rehabil Eng* 14(2):190–193
15. Kronegg J, Chanel G, Voloshynovskiy S, Pun T (2007) EEG-Based synchronized brain-computer interfaces: a modal for optimizing the number of mental tasks. *IEEE Trans Neural Syst Rehabil Eng* 15:50–58

16. Naeem M, Brunner C, Leeb R, Graimann B, Pfurtscheller G (2006) Separability of four-class motor imagery data using independent component analysis. *J Neur Eng* 3(3):208–216
17. Mahmoudi B, Erfanian A (2006) Electro-encephalogram based brain-computer interface: improved performance by mental practice and concentration skills. *Med Biol Eng Comput* 44(11):959–69
18. Munk F (2000) Introduction to joint time-frequency analysis, Compendium for the course, Aalborg University, Denmark, pp 69–80
19. Navarro I, Sepulveda F, Hubais B (2005) A comparison of time, frequency and ICA based features and five classifiers for wrist movement classification in EEG signals. In: Proceedings of 27th IEEE engineering EMBS conference, Shanghai, pp 2118–2121
20. Neuper C, Scherer R, Reiner M, Pfurtscheller G (2005) Imagery of motor actions: differential effects of kinesthetic and visual-motor mode of imagery in single-trial EEG. *Brain Res Cogn Brain Res* 25(3):668–677
21. Onton J, Makeig S (2006) Information-based modeling of event-related brain dynamics. *Prog Brain Res Elsevier* 159:99–134
22. Palaniappan R (2006) Utilizing gamma band to improve mental task based brain-computer interface design. *IEEE Trans Neural Syst Rehabil Eng* 14(3):299–303
23. Pfurtscheller G, Brunner C, Schlogl A, Lopes da Silva FH (2006) Mu rhythm (de)synchronization and EEG single-trial classification of different motor imagery tasks. *Neuroimage* 31(1):153–159
24. Pfurtscheller G, Neuper C (2006) Future prospects of ERD/ERS in the context of brain-computer interface (BCI) developments. *Prog Brain Res Elsevier* 159:433–7
25. Qian S, Chen D (1996) Joint time-frequency analysis: methods and applications. Prentice Hall
26. Ramoser H, Muller-Gerking J, Pfurtscheller G (2000) Optimal spatial filtering of single trial EEG during imagined hand movement. *IEEE Trans Rehabil Eng* 8(4):441–446
27. Sepulveda F, Meckes M, Conway BA (2004) Cluster separation index suggests usefulness of EEG non-motor channels in detecting wrist movement direction intention. In: Proceedings of IEEE ICS'04, Singapore, vol 2, pp 943–947
28. Stanstny J, Sovka P, Stancak A (2001) EEG signal classification. In: Proceedings of 23rd international EBMS annual conference, pp 220–223
29. Talsma D, Woldorff MG (2005) Methods for the estimation and removal of artifacts and overlap in ERP waveforms, in event-related potentials. A method handbook, The MIT Press, pp 115–149
30. Townsend G, Graimann B, Pfurtscheller GA (2006) A comparison of common spatial patterns with complex band power features in a four-class BCI experiment. *IEEE Trans Biomed Eng* 53(4):642–651
31. Vidaurre C, Schlogl A, Cabeza R, Scherer R, Pfurtscheller G (2006) A fully on-line adaptive BCI. *IEEE Trans Biomed Eng* 53(6):1214–1219
32. Vučković A, Sepulveda F (2006) EEG single-trial classification of four classes of imaginary wrist movements based on Gabor coefficients. In: Proceedings of 3rd international BCI workshop, Graz, Austria, pp 26–27
33. Vučković A, Sepulveda F (2008) Quantification and visualisation of differences between two motor tasks based on energy density maps for brain computer interface applications. *Clin Neurophysiol* 119(2):446–458
34. Wang G, Wang Z, Chen W, Zhuang J (2006) Classification of surface EMG signals using optimal wavelet packet method based on Davies-Bouldin criterion. *Med Biol Eng Comp* 44:865–872
35. Zygierevicz J, Durka PJ, Klekowicz H, Franaszczuk PJ, Crone NE (2005) Computationally efficient approaches to calculating significant ERD/ERS changes in the time-frequency plane. *J Neurosci Methods* 145(1–2):267–76